3D Countersink Measurement

Ryan Haldimann
Electroimpact, Inc.

Abstract

Accurate measurement of countersinks in curved parts has always been a challenge. The countersink reference is defined relative to the panel surface which includes some degree of curvature. This curvature thus makes accurate measurements very difficult using both contact and 2D non-contact measurements. By utilizing structured light 3D vision technologies, the ability to very accurately measure a countersink to small tolerances can be achieved. By knowing the pose of the camera and projector, triangulation can be used to calculate the distance to thousands of points on the panel and countersink surface. The plane of the panel is then calculated using Random Sample Consensus (RANSAC) method from the dataset of points which can be adjusted to account for panel curvatures. The countersink is then found using a similar RANSAC method. As the full geometric definition of the countersink and the plane are known, the radius and angle of the countersink can be calculated by intersecting of the two geometries to find the countersink diameter and depth. By inspecting the fit of each set of point to their respective geometric entities a confidence factor can be generated for the overall countersink measurement. Utilization of this technique would allow for more detailed measurement of countersink features.

Introduction

The objective was to investigate using structured light scanning system to capture and analyze 3D data to measure a countersink. Measurements made by edge finding were shown by Webb et al(1) using direct illumination and Meiners (2) using an off axis laser projector. Both methods did not have a quality measure nor directly measure normality.

Non-Contact Techniques

To utilize a single camera image capture that will collect 3D point data an illumination system would be required. Lasers, Structured Light LED, and Projectors are some of the non-contact techniques applicable to the aforementioned task.
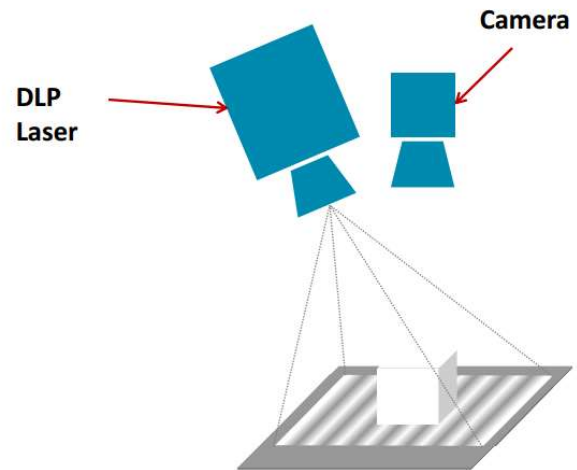

Figure 1. Camera Projector Setup

Furthermore, using a laser line for illumination requires part-camera movement to achieve full countersink definition. Subsequently this introduces additional inaccuracies and significantly increases data acquisition time, rendering the practical application of this method inadequate. Conversely, a fixed Digital Light Processing (DLP) projector allows a 2D series of Gray code patterns to be overlaid on the part with high enough resolution and no machine motion to achieve proper measurement. This allows for triangulation of each ray from the camera to be intersected with each ray from the projector, providing a full surface cloud of data.
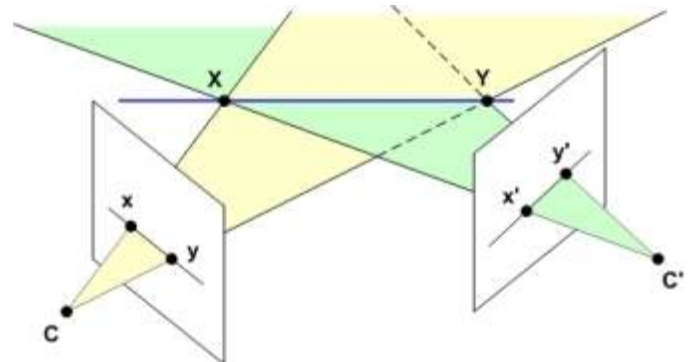

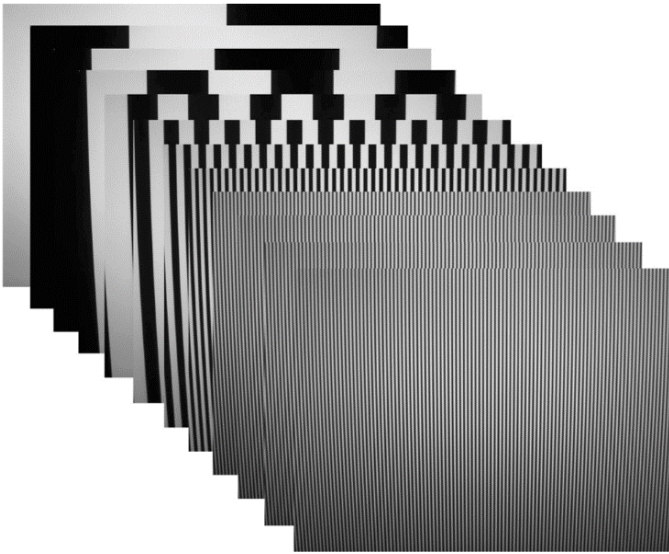Figure 2. Camera Projector Triangulation

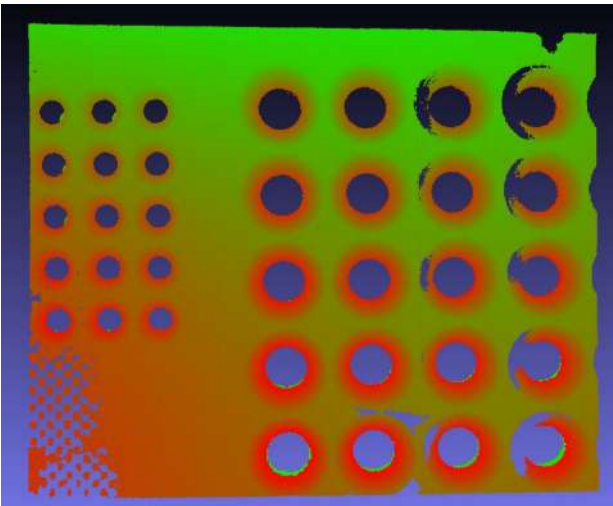Figure 3. Gray Encoding

Point Cloud Capture Using Structured Light

Figure 4. Point Cloud Dataset

Hardware

A TI DLP projector and USB camera were arranged on a test bench and secured as illustrated in Figure 6.

Figure 5. TI DLP Projector

Efficacy Factors

There are a number of factors that can affect the dataset quality including material surface finish, material type, surface contamination and the geometry of the imaging setup.

Primary among these factors is the material type. A metallic material countersink will only display directly reflected light and without using HDR imaging techniques a viable image is unable to be obtained. The standard countermeasure to glare would be the use of a polarizer however they are unable to be employed, as metal, unlike all other materials, does not cause polarization. Similarly polarizing the light source does not provide any benefit as the glare can be reduced in levels but the countersink portion is still unable to be imaged. Non Metallic materials, namely composites, provide acceptable results in the raw material of the countersink.

A satisfactory surface finish is required as determination of the surface plane would not be able to be determined with inadequate data. Painted or OML composite generate better data than IML composite as the light is not directly reflected and produces better data.

Surface contamination w cutting fluids, swarf or sealant can also negatively affect data acquisition. Dry clean parts yield the best result but are rarely encountered during in process inspection.

Point cloud data accuracy is directly related to imaging geometry. Specifically the resolving power is inversely proportional to the camera and projector angles by the relationship in equation 1, where X_c is camera accuracy in pixels, R_c is camera resolution in pixels,
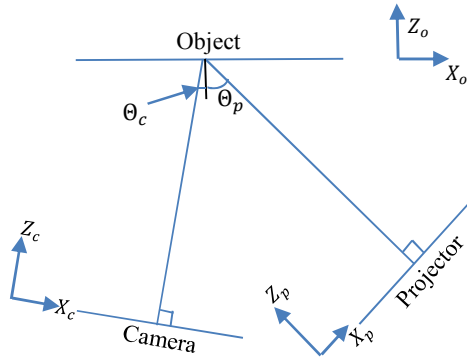
FOV_c is the Field of View of the camera.

$$Z_o = \frac{X_c * \frac{R_c}{FOV_c}}{\tan(\Theta_p) * \cos(\Theta_c)} \quad (1)$$

Point Cloud Analysis

Processing Pipeline

Once the data is acquired and filtered, an appropriate region is selected for analysis based on predetermined constraints such as part curvature and adjacent fasteners. Sequential operations are applied to the data to isolate the countersink and its intersection to the surface plane it is to be measured against.
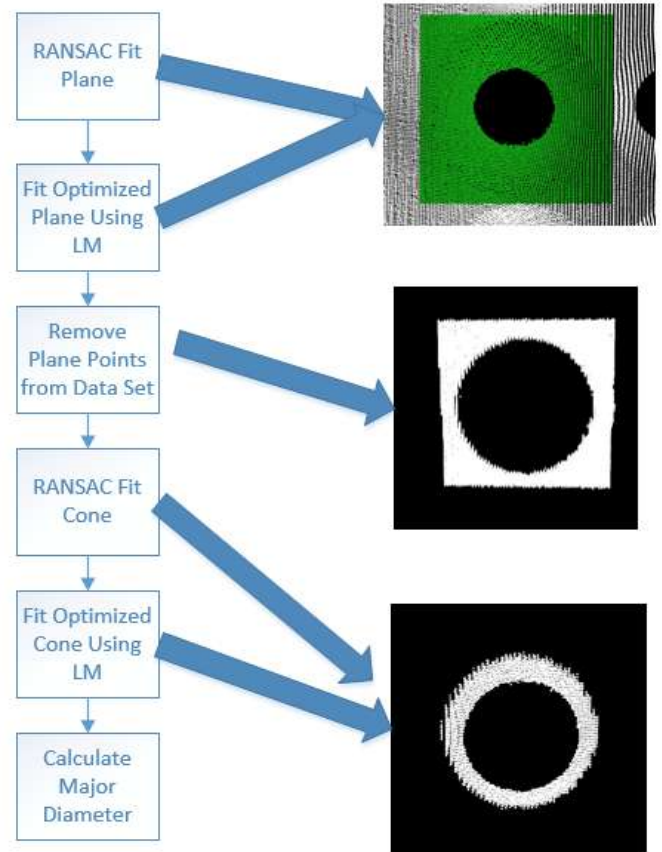

Figure 7. Processing Pipeline

Determining Reference Plane

Random Sample Consensus (RANSAC) is used to find a plane fitting a portion of the data set. RANSAC algorithms operate by selecting a set of points randomly from the dataset and fitting the desired type of model to these points. All points in the dataset within some tolerance of this model definition are then counted. The algorithm then continues until a number of statistical measures are satisfied, whether it's the count of selected points or the number of searches. The points falling within the tolerance are then optimized using Levenberg Marquardt (LM) algorithms, a gradient decent method of solving non-linear least squares problems, to return optimized plane parameters consisting of the cone apex, direction and included angle.

Subtracting Plane Points from Data Set

The cone points are isolated from the dataset by subtracting the points defined within some tolerance of the reference plane. Using a tolerance larger than that used to calculate the plane is required so that only points representing the cone are selected.

Finding Countersink Circle

The points in the data set corresponding to the plane definition are then searched using RANSAC tools for a circle with nominal radius. The circle parameters are optimized using LM techniques.

Fitting a Cone

Initial cone parameters are estimated from the circle radius, location and default cone angle. To accelerate cone finding the normal for each point is estimated by first sorting the points into a K-Dimensional tree then using the cross product of the Eigenvectors for points lying within a defined radius of the target point as described by Rusu (3). The cone parameters are then optimized using LM algorithms.

Calculating Major Diameter of Cone Intersection

To calculate the Major Diameter of the Ellipse created by the Cone and Plane intersection, the cross product of the cone axis and the plane axis create a vector $(\overrightarrow{P_{mn}})$ perpendicular to the major axis. The cross product of $\overrightarrow{P_{mn}}$ with the plane normal creates $\overrightarrow{P_{mx}}$ in the direction of the major axis. Points of intersection between a vector emanating from the cone apex and extending at the cone angle (in both directions) and the major axis vector is then calculated. The countersink major diameter (C_{md}) is the distance between the intersection points (I_{c1}, I_{c2}). The angle of the countersink is calculated using the cosine of the dot product of the plane normal vector and the cone direction vector.
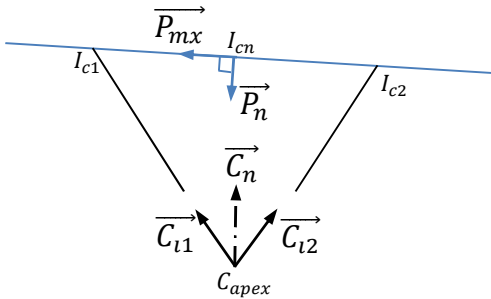

Figure 8. Countersink Major Diameter Calculation

$$I_{c1} = C_{apex} + \frac{(I_{cn} - C_{apex}) \times \overrightarrow{P_{mx}}}{\overrightarrow{C_{l1}} \times \overrightarrow{P_{mx}}} * \overrightarrow{C_{l1}} \quad (2)$$

$$I_{c2} = C_{apex} + \frac{(I_{cn} - C_{apex}) \times \overrightarrow{P_{mx}}}{\overrightarrow{C_{l2}} \times \overrightarrow{P_{mx}}} * \overrightarrow{C_{l2}} \quad (3)$$

$$C_{md} = \|I_{c1} - I_{c2}\| \quad (4)$$

$$\Theta_{csk} = \cos^{-1}\left(\frac{\overrightarrow{C_n} \cdot \overrightarrow{P_n}}{\|\overrightarrow{C_n}\| * \|\overrightarrow{P_n}\|}\right) \quad (5)$$

Results

The method outlined herein provides a robust means for calculating the countersink diameter and angle and provides the benefit of a fit value so that confidence in the measurement can be evaluated. Using the above techniques a measurement standard deviation of 0.0012"

was obtained compared to CMM measurements. Cone fit residuals for noisy data sets was on the order of 0.005mm/point where a fit that achieved the above measurement accuracy results were 0.001mm/point.

Summary/Conclusions

Fitting geometry to point clouds for measurement allows for higher confidence in the measurement. If the countersink is contaminated by swarf or coolant the residuals for a fit to geometry increase allowing an acceptance threshold to be set, ruling out erroneous results. The aforesaid techniques describe a robust method for measurement of countersinks on nonmetallic surfaces.

References

1. Webb, P., Chitiu, A., Khalili, K., and McKeown, C., "Vision Based In-Process Inspection for Robotic Automated Riveting," SAE Technical Paper 2004-01-2819, 2004, doi:10.4271/2004-01-2819
2. Meiners, C., "Advances in Automated Inspection Using Contactless Head Height and Countersink Measurement Techniques," SAE Int. J. Mater. Manf.7(1):33-36, 2014, doi:10.4271/2013-01-2148.
3. Rusu, R, "Semantic 3D Object Maps for Everyday Manipulation in Human Living Environments", Dissertation 2009, Technical University of Munich

Definitions/Abbreviations

RANSAC	Random Sample Consensus algorithm
DLP	Digital Light Processing
HDR	High Dynamic Range
KD Tree	K Dimensional Tree used to organize points
LM	Levenberg Marquardt algorithm
Swarf	fine chips or filings of stone, metal, or other material produced by a machining operation.